



**Acoustics'08
Paris**
June 29-July 4, 2008

www.acoustics08-paris.org

euonoise

Sonar target-phase measurement and effects of transducer-matching

Philip Atkins^a, Alan Islas^a and Kenneth Foote^b

^aUniversity of Birmingham, Department of Electronic, Electrical and Computer Engineering,
Edgbaston, B15 2TT Birmingham, UK

^bWoods Hole Oceanographic Institution, Woods Hole, MA 02543, USA
p.r.atkins@bham.ac.uk

Active sonar systems normally detect and classify a target based on the amplitude of the received echo or the induced Doppler shift. However, additional classification information may be available from the phase shift introduced by some targets as a result of the boundary conditions. For example, reverberation from the sea surface and scattering from fish swimbladders introduce an additional phase shift that may not be present in returns from an acoustically stiffer seabed or synthetic target. Algorithms based on the use of sub-band correlators are presented for measuring the phase shifts introduced by the boundary conditions on stationary and moving targets when insonified by broadband transmissions. These techniques are used to remove the phase shifts introduced by the unknown target. However, the unknown phase characteristics of the transducer, matching circuit, and electronic circuitry of a sonar system imply that target-phase measurements are very difficult to conduct in any practical system. The effects of adding a Butterworth-derived matching circuit to a Reson TC2130 transducer are presented for the case of sinusoidal frequency-modulated excitation of solid elastic and thin elastic-shelled hollow spheres. It is concluded that target-phase measurements can enhance the classification performance of a suitably calibrated sonar system.

1 Introduction

Active sonar systems normally detect and classify a target based on the amplitude of the received echo strength or the induced Doppler shift. However, additional classification information is available from the phase shift introduced by some targets as a result of the boundary conditions. For example, reverberation returns from the sea surface and from the swimbladders of various fish introduce an additional phase shift that may not be present in returns from an acoustically stiffer seabed or man-made target. The measurement of target-phase is complicated by the additional phase shifts introduced by the unknown target range and by the phase shifts introduced by Doppler as a result of target and platform motion. Typically, target-phase is estimated by insonifying the target with a signal that contains at least two frequency-scaled components. Thus a more complicated received structure is required that contains a full-band correlator for detection purposes and sub-band correlators for estimating target-phase.

Unfortunately, the unknown phase characteristics of the transducer and electronic circuitry of a sonar system add significantly to the difficulties of target-phase measurements. Calibration procedures based on the use of standard targets normally address only the magnitude response of a system. However, such techniques may be extended to estimate the phase response of a sonar system by the use of suitable transmission signal types. This paper derives two transmission pulse types suitable for measuring target-phase in conjunction with sub-band correlators and presents experimental results for solid standard elastic target spheres and thin elastic-shelled hollow spheres. These experimental results were obtained using a Reson TC2130 transducer operating at a nominal frequency of 100 kHz. The implications of using a transducer without regard to the effects of power amplifier-transducer impedance matching are demonstrated followed by the improvements derived from adding a Butterworth and Bessel-derived matching circuit.

2 Target-phase Measurement

Consider the case of an incident pressure wave generated by a sonar system and described by $p_{inc} = P_{inc} \exp[j(\omega t - k_A r)]$ where P_{inc} is the peak incident pressure, ω is the operating frequency, t is time,

k_A and k_B are the wavenumbers associated with the media on either side of the encountered boundary, and r is the range from the transmitter, as shown in Fig. 1. A reflected wave $p_R = P_R \exp[j(\omega t - 2k_A r_0 + k_A r)]$ and a transmitted wave $p_T = P_T \exp[j(\omega t - k_A r_0 - k_B (r - r_0))]$ will be generated where P_R is the peak reflected pressure, P_T is the peak transmitted pressure, r_0 is the range to the boundary wall of the target and collinear geometry is assumed. Assuming planar boundary areas and plane wave insonification, the reflection and transmission coefficients can be extracted

$$R = \frac{\rho_B c_B - \rho_A c_A}{\rho_B c_B + \rho_A c_A} \quad T = 1 + R = \frac{2\rho_B c_B}{\rho_B c_B + \rho_A c_A} \quad (1)$$

where ρ represents the density of the material, c is the sound speed, and ρc is the acoustic impedance of the material.

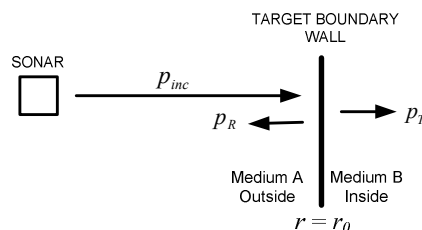


Fig. 1. Target at range r_0 insonified by an incident wave

It will be noted that if the acoustic impedance of medium B ($\rho_B c_B$) is less than that of medium A ($\rho_A c_A$), the reflection coefficient will be negative. This implies that for a monostatic sonar system there will be a π -rad phase change occurring for all transmission frequencies whenever the target is acoustically soft. No phase change will be encountered if the target is acoustically hard.

The first reference to measuring target-phase in the field appears to be by Tucker and Barnicle [1], who insonified a target using two harmonically related frequencies and compared the relative phases of the backscattered signals in order to provide additional detection information for the characterisation of fish containing swimbladders. Their technique involved transmitting a low-frequency sinusoidal signal, $p_1 = P_1 \exp(j\omega_1 t)$, and a higher-frequency signal,

$p_2 = P_2 \exp(j\omega_2 t)$, where P_1 and P_2 are the peak pressures of the two transmitted components. If the target is located at a range r and introduces a phase shift ϕ , then the

pressure at the receive hydrophone (assuming identical outward and return propagation paths) is proportional to

$$p_{RX} = P_1 \exp[j(\omega_1 t - 2k_1 r + \phi)] + P_2 \exp[j(\omega_2 t - 2k_2 r + \phi)] \quad (2)$$

where k_1 and k_2 are the associated wavenumbers in the water of the low and high frequency signals. The higher-frequency signal will have some fixed relationship to the low-frequency signal, such that $\omega_2 = \mu \omega_1$. Tucker and Barnicle [1] chose a harmonic relationship with $\mu = 2$. The phase comparison of the two received signal components must be made at a common frequency and this was chosen to be that of the higher-frequency signal, ω_2 . The receiver structure must isolate the two transmission signals using sub-band processors to generate output signals that are band-limited about centre frequencies ω_1 and ω_2 . The phase comparison of the two sub-band transmissions is achieved by frequency-scaling the component corresponding to the time-varying pressure p_1 by the factor μ to obtain a signal

$$p_{Scaling} = \left\{ P_1 \exp[j(\omega_1 t - 2k_1 r + \phi)] \right\}^\mu = P_1^\mu \exp[j\mu(\omega_1 t - 2k_1 r + \phi)] \quad (3)$$

The phase comparison is achieved by multiplying the signal $p_{Scaling}$ and the complex-conjugate signal of the higher-frequency transmission component p_2^* .

$$p_{Scaling} p_2^* = P_1^\mu \exp[j\mu(\omega_1 t - 2k_1 r + \phi)] P_2 \exp[-j(\omega_2 t - 2k_2 r + \phi)] \quad (4) = P_1^\mu P_2 \exp[j(\mu - 1)\phi]$$

The phase comparison operation generates a signal with a purely real amplitude term $P_1^\mu P_2$ that will be ignored and a complex term $\exp[j(\mu - 1)\phi]$ whose argument is proportional to the phase shift introduced by the target. The phase shifts introduced by $\exp[j(\omega t - 2kr)]$ due to the time-varying nature of the transmission signal and the unknown target range have been cancelled. The phase term $\exp[j(\mu - 1)\phi]$, introduced by the target, is related to the separation between the centre frequency of the two sub-bands and any practical implementation should ensure that the value of μ is made as large as possible to reduce the effects of phase noise.

The phase comparison process takes a sinusoid, $\exp[j(\omega_1 t + n2\pi)]$ with an unknown phase origin, where n is an integer, and scales it to a higher-frequency, $\exp[j\mu(\omega_1 t + n2\pi)]$. The phase of this signal is compared to a higher-frequency signal $\exp[j(\omega_2 t + l2\pi)]$, where l is an integer. The resulting phase difference is $(2\pi\mu n) \bmod 2\pi$ which could assume any value. However, the phase difference should be constrained to be part of a finite set of values corresponding to permissible phase sectors. Assuming that M permissible phase sectors are to be used in a system, then $(2\pi\mu nM) \bmod 2\pi = 0$, or $(\mu nM) \bmod 1 = 0$ where M

is an integer and $\mu > 1$. The constraint on the ratio of the centre frequency of the two sub-bands, μ , is

$$\mu = \frac{M + N}{M} \text{ where } N \text{ is an integer and } N \geq 1. \quad (5)$$

In order to conserve bandwidth, an appropriate value of μ , usually chosen from the set $\mu = [2, 3/2, 4/3, 5/3, 5/4, 7/4]$, would be selected from which it can be deduced that an acoustically hard target echo will fall into one of the $N/(\mu - 1)$ hard-phase sectors, whilst a soft target will fall into one of the $N/(\mu - 1)$ soft-phase sectors. An additional phase-modulus operation would be used to roll all the received phase samples into a single hard-phase sector, or a single soft-phase sector prior to any decision process.

The block diagram of a typical active sonar system used to measure target-phase is shown in Fig. 2. The transmission signal with identifiable information content at frequencies of ω_1 and ω_2 is stored in a look-up table. The received signal is full-band correlated in a conventional manner for target detection purposes. The received signal is also sub-band processed using two correlators, each having the dual-function of optimising the signal-to-noise ratio and ensuring a symmetrical spectral content about the sub-band frequencies in order to obtain components at ω_1 and ω_2 . The correlator coefficients are obtained by judicious weighting of the transmission signal. The highest-frequency sub-band (Band 2) is used as the reference channel, whilst the lowest-frequency sub-band (Band 1) is frequency-scaled prior to phase comparison with the reference channel. The use of sub-octave frequency separations introduces ambiguities within the phase measurement process, which, following a careful design approach based on choosing $\mu = [2, 3/2, 4/3, \dots]$, will be limited to a finite number of phase sectors. This ambiguity is resolved in conjunction with the output decision process in order to provide a hard-soft decision corresponding to every range cell.

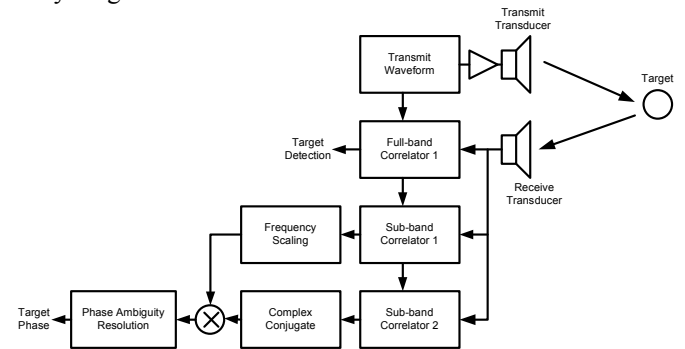


Fig. 2. Block diagram of target-phase estimation sonar

3 Possible Transmission Signals

The majority of transmission signals that contain identifiable spectral components at two discrete frequencies may be used for target-phase estimation. Examples included within this section are pulsed continuous wave (CW) and hyperbolic frequency-modulated (HFM). Generally, signals with poor range-resolution capabilities such as CW and sinusoidal frequency-modulated (SFM) [2] would be used for calibration purposes whilst signals such as HFM would be used for operational purposes.

3.1 Pulsed Continuous Wave (CW)

A pulsed CW signal may be described by

$$s(t) = A(t) \exp(j\omega_k t) \quad (6)$$

where $A(t)$ is the amplitude window function and will initially be assumed to be rectangular $A(t) = \text{rect}(t/T)$, k is the sub-band index and the signal is active in the region $-T/2 \leq t \leq T/2$. The receiver would be based on the FFT algorithm in order to implement a bank of Doppler-matched filters to measure target velocity whilst maintaining detection performance. In a typical operating scenario, a large number of Doppler-shifted propagation paths will be received within a short period of time. Thus the matched filter is always likely to be Doppler-mismatched and the effects of this mismatch should be considered on the performance of the hard-soft estimation technique.

The output of a Doppler-matched filter can be described as

$$\varphi_{xy}(\tau) = \int x(t+\tau) y^*(t) dt \quad (7)$$

where $x(t+\tau)$ is assumed to be the received signal and $y^*(t)$ is assumed to be the complex conjugate of the replica signal.

Consider the case of one of the sub-band correlators acting on a pulsed, Doppler-shifted CW signal. The analytic signal description of an infinite-extent received signal time-compressed or expanded by an unknown Doppler factor, η , will be $x(t) = \sqrt{\eta} \exp(j\omega\eta t)$ and the complex conjugate infinite-extent replica will be $y^*(t) = \exp(-j\omega t)$. In a practical implementation, the length of the replica used in the receiver will be shorter than the transmitted signal to partially reduce the effects of Doppler overlap losses and to ensure that the receiver determines the spectral content of the processed signals. Thus the limits of the matched filter integration will be $-T/2 \leq t \leq +T/2$ where T is the receiver replica length

$$\varphi_{xy}(\tau, \eta) = \sqrt{\eta} \int_{-T/2}^{+T/2} \exp(j\omega\eta(t+\tau)) \exp(-j\omega t) dt \quad (8)$$

$$\varphi_{xy}(\tau, \eta) = \sqrt{\eta} T \exp(-j\omega\eta\tau) \text{sinc}(\omega T(1-\eta)/2). \quad (9)$$

The propagation delay is τ . Eq.(9) represents the ambiguity function for an infinite-extent Doppler-mismatched CW signal correlated against a replica of a pulse, using the centre of the replica as the time reference. The envelope remains constant for a change in the range of the target (variations in the value of τ) and varies as a sinc function for changes in the Doppler shift function η . The important parameter to note is the phase shift associated with $\exp(-j\omega\eta\tau)$, which is linearly related to the centre-frequency of the sub-band, ω . Thus calculating the phase of the Doppler-mismatched received signals at two sub-band frequencies and comparing the results will lead to the elimination of the $\exp(-j\omega\eta\tau)$ term.

It can be seen that the phase shifts introduced by Doppler effects and varying ranges within a multi-path cluster are not coupled to the target-induced phase shifts when using a pulsed, dual-frequency, CW signal. The CW signal, or

adaptations of it such as the Cox comb [3], represents a good choice of transmission signal for estimating the phase characteristics of the target in a multi-path, Doppler-spread environment, although the range-resolution is normally unacceptably poor because of the limited bandwidth utilisation.

3.2 Hyperbolic Frequency-Modulated

Hyperbolic frequency-modulated signals are often classed as Doppler tolerant because the amplitude of the matched filter response only marginally decreases as a function of target velocity. This Doppler tolerance allows the designer to use a single-correlator receiver implementation. Unfortunately, the Doppler amplitude tolerance of HFM transmissions results in Doppler-induced phase variations that couple to the target-phase and cannot be resolved using a single transmission.

The transmitted signal may be written in the form [4]

$$s(t) = A(t) \exp\left(\frac{j}{b} \ln(1+b\omega_l t)\right) \quad 0 \leq t \leq T \quad (10)$$

where $A(t)$ is the transmit signal window function. The variable $b = (1/\omega_f - 1/\omega_l)/T$ defines a unique sweep factor where ω_l is the start frequency of the transmission sweep, ω_f is the end frequency of the transmission sweep and T is the duration of the transmission sweep.

If the transmitted signal is time-compressed by a factor η , such that the received signal is expressed as $s_R(t) = \sqrt{\eta} s(\eta t)$, then the output of the receiver may be expressed as [4]

$$s_R(t) = \sqrt{\eta} A(\eta t) \exp\left(\frac{j2\pi}{b} \ln\left(1 + \frac{b}{T}(t-t_D)\right) + j\phi_D\right). \quad (11)$$

The received signal is subject to a constant time delay $t_D = (\eta-1)/(\eta\omega_l b)$ and a constant phase shift $\phi_D = \ln(\eta)/b$. The target-phase measurement process uses two sub-bands separated by a frequency ratio of μ . Thus the phase difference between the two sub-band correlator outputs is

$$\theta_{HS} = \frac{(\mu-1)}{b} \ln(\eta) + (\mu-1)\phi \quad (12)$$

where ϕ is the phase shift imparted by the target. The phase shift imparted by a Doppler shift and by the target are thus directly coupled. The Doppler-induced phase shift cannot be removed simply as the frequency sweep parameter, b , is fixed for a given single-sweep transmission.

However, the simultaneous transmission of two HFM signals [5] with respective sweep rates of b_1 and b_2 results in a phase difference between the two sub-band correlator outputs of

$$\theta_{HS} = \left(\frac{\mu}{b_1} - \frac{1}{b_2}\right) \ln(\eta) + (\mu-1)\phi. \quad (13)$$

It will be noted that by ensuring that $b_1 = \mu b_2$ the Doppler effects can be cancelled, this results in the desired output of $\theta_{HS} = (\mu-1)\phi$.

4 Transducer characteristics

With the exception of inter-element matching in transducer arrays, the effects of phase are rarely considered within a sonar system. Consider the simplest of electrical-analogue models [6] for a transmit transducer operating near resonance, as illustrated in Fig. 4. The radiation and loss resistance is combined and represented by R_{rad} . The motional impedances are represented by L_{mot} and C_{mot} , whilst the shunt capacitance is represented by C_s . When operated in a transmit mode, a matching circuit would be added to cancel the reactive part of the input impedance thus providing a more favourable load for the power amplifier. Such matching circuits are traditionally designed using a band-pass filter assumption, in order to improve the response characteristics of the transducer [6, 7, 8]. The specific goals for the present work are to increase the bandwidth to obtain more information from the received signal, and also, to linearise the phase response, in order to be able to identify phase shifts introduced by the target for the previously described classification algorithm.

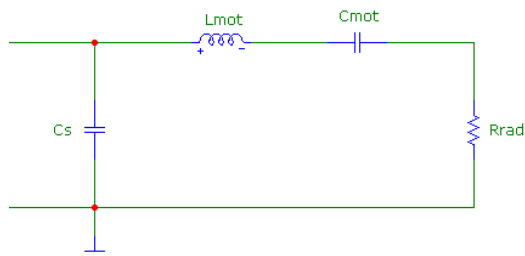


Fig 4. Classical transducer equivalent circuit

4.1 Filter-derived transducer matching

Admittance measurements were made for a Reson TC2130 transducer, using a HP4291A impedance analyzer. The experimental data was then fitted to the model shown in Fig. 4 to yield the values of the equivalent electrical components, by means of a simplex minimization routine. The frequency range was limited to that of the main resonance in order to avoid the effects of multiple resonances within the transducer, as illustrated in Fig. 5.

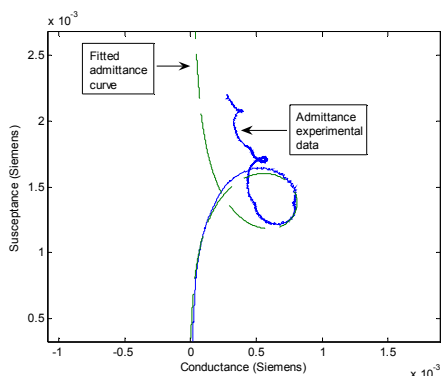


Fig 5. Experimental and model admittance loops.

The electrical model obtained from the measurements plotted in Fig. 5 is shown in Fig. 6.

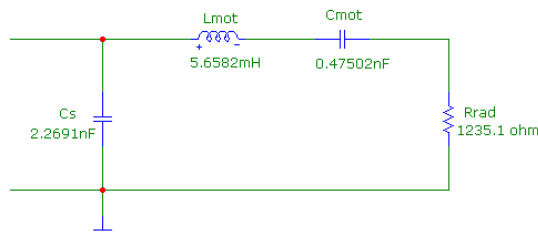


Fig.6 Equivalent circuit of a Reson TC2130 transducer.

The transducer and the electronic circuitry associated with the sonar system add a phase shift that equates to a frequency-dependent time delay, thus distorting the shape of the received waveform. Both Butterworth and Bessel-derived transducer matching circuits were investigated with the objectives of linearising the phase shift and increasing the system bandwidth.

The design of a double-terminated Butterworth and Bessel, 3rd order band-pass networks were based on standard design methods [9, 10], and the resulting circuits (Figs. 7a and 7b), connected to the transducer equivalent circuit, were analysed, simulated and measured.

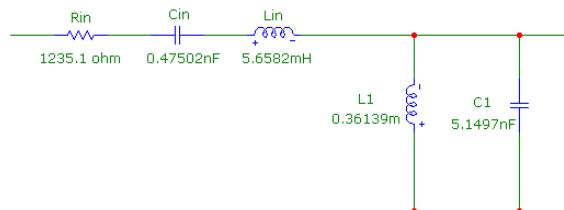


Fig. 7a. Butterworth-derived matching circuit

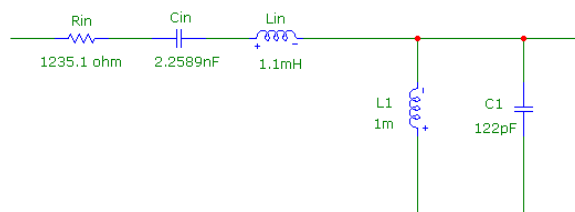


Fig. 7b. Bessel derived matching circuit

The measured and predicted admittance data obtained for the Butterworth and Bessel matching circuits is illustrated in Figs. 8 and 9.

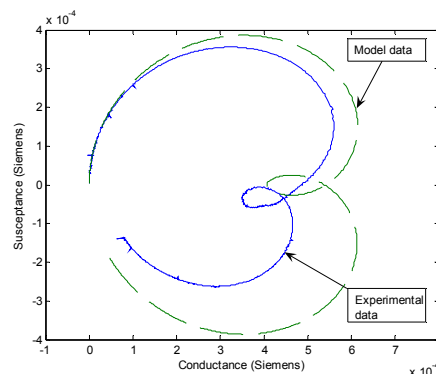


Fig. 8. Butterworth matching admittance loops

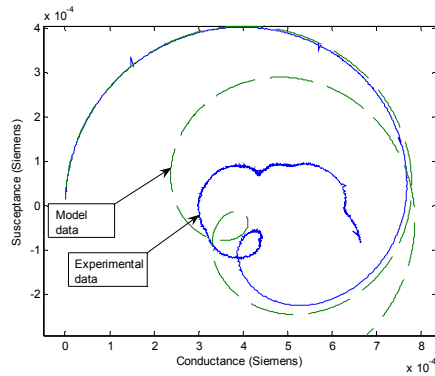


Fig 9. Bessel matching admittance loops

The performance comparison between the two matching schemes and the unmatched transducer was performed in terms of bandwidth and phase linearity. The three amplitude transfer functions, with their -3 dB points marked, are illustrated in Fig. 10.

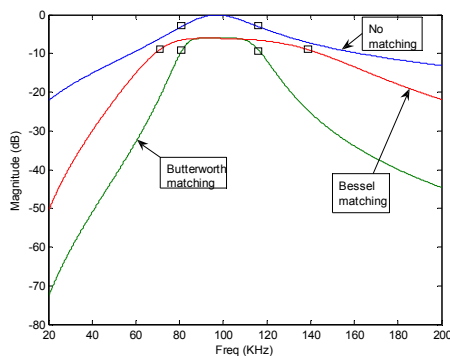


Fig. 10. Predicted amplitude transfer functions

It can be observed that the unmatched transducer, and the Butterworth matched transducer have approximately the same bandwidth, about 35 kHz; while the Bessel matching transfer function increases the bandwidth to approximately 68 kHz.

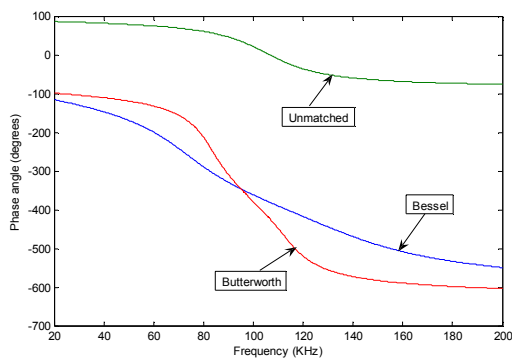


Fig. 11. Phase response

From Fig. 11, it can be clearly seen that the Bessel exhibits a response that is approximately linear over a larger frequency range; as this was designed to obtain a maximally flat phase response. Classical transducer texts, such as Stansfield [6], have primarily focused on the efficient transfer of power and the enlargement of bandwidth, without taking phase into consideration. Chen [11] adopts a powerful mathematical approach to the problem, although it is not known if this approach has been applied in the underwater acoustics environment.

Lack of space within this paper precludes the inclusion of corroborative acoustic measurements using standard acoustic targets – to be presented during the conference.

5 Conclusion

The concept of using a dual-frequency transmission signal to measure the phase response of a target has been introduced. Transmission signal types such as hyperbolic frequency-modulated chirps may be adapted for measuring target-phase whilst maintaining good range resolution. However, it is essential that the phase characteristics of the sonar system are measured and compensated before such techniques have any practical use. The use of transducer matching circuits optimised for linear phase characteristics has been shown.

References

- [1] D.G. Tucker and N.J. Barnicle, "Distinguishing automatically the echoes from acoustically 'hard' and 'soft' objects with particular reference to the detection of fish," *J. Sound Vib.* 9, pp. 393-397, May 1969.
- [2] T. Collins and P.R. Atkins, "Doppler-sensitive active sonar pulse designs for reverberation processing," *IEE Proc. Radar, Sonar Navig.*, Vol. 145, pp. 347-353, December 1998.
- [3] H. Cox and H. Lai, "Geometric comb waveforms for reverberation suppression," *Proceedings of the Twenty-Eighth Asimolar Conference on Signal, Systems and Computers*, Vol. 2, pp. 1154-1189, October 1994.
- [4] J.J. Kroszczynski, "Pulse Compression by Means of Linear Period Modulation," *Proc. IEEE*, Vol.57, No. 7, pp. 1260-1266, July 1969.
- [5] P.R. Atkins, T. Collins, and K.G. Foote, "Transmit-signal Design and Processing Strategies for Sonar Target Phase Measurement," *Proc. IEEE Selected Topics in Signal Processing*, Vol.1, No. 1, pp. 91-104, June 2007.
- [6] D. Stansfield, "Underwater Electroacoustic Transducers," Bath University Press, 1991.
- [7] P.E. Doust and J.F. Dix, "The impact of improved transducer matching and equalisation techniques on the accuracy and validity of underwater acoustic measurements," *Proc. Institute of Acoustics Volume 23, Pt2*, 2001, 100-109. ISBN 1901 656 34 9.
- [8] P.E. Doust, "Method and apparatus for equalizing transfer functions of linear electro-acoustic systems," Patent No. W) 01/83122 A1, 2001.
- [9] W.K. Chen, "The circuits and filters handbook," Boca Raton, Florida, CRC Press, 1995.
- [10] L.P. Huelsman, "Active and passive analog filter design," New York, McGraw Hill, 1993
- [11] Y.S. Zhu, W.K. Chen, "Broad-band matching with maximally flat group delay characteristics," *IEEE Transactions on Circuits and Systems*, Vol. 34, No. 6, pp. 658-668, June 1987.